

Supporting Information

Three new super water-stable lanthanide–organic frameworks for luminescence sensing and magnetic properties

Wen-Quan Tong,^a Ting-Ting Liu,^b Gao-Peng Li,^a Ji-Ye Liang,^a Lei Hou^a, and Yao-Yu Wang^{*a}

Key Laboratory of Synthetic and Natural Functional Molecule Chemistry of the Ministry of Education, Shaanxi Key Laboratory of Physico-Inorganic Chemistry, College of Chemistry and Materials Science, Northwest University, Xi'an, Shaanxi 710127, P. R. China. E-mail: lhou2009@nwu.edu.cn; E-mail: wyaoyu@nwu.edu.cn.

Table S1. Selected bond lengths (Å) and bond angles (deg) for complex **1-Eu**, **1-Tb** and **1-Dy**.

1-Eu			
Eu(1)-O(7)#1	2.302(7)	O(1)-Eu(1)-O(3)#3	91.8(3)
Eu(1)-O(8)#2	2.329(7)	O(1W)-Eu(1)-O(3)#3	92.7(4)
Eu(1)-O(1)	2.378(7)	O(7)#1-Eu(1)-O(4)#3	75.1(3)
Eu(1)-O(1W)	2.420(8)	O(8)#2-Eu(1)-O(4)#3	140.6(3)
Eu(1)-O(3)#3	2.471(9)	O(1)-Eu(1)-O(4)#3	128.4(3)
Eu(1)-O(4)#3	2.475(8)	O(1W)-Eu(1)-O(4)#3	75.3(3)
Eu(1)-O(3W)	2.485(8)	O(3)#3-Eu(1)-O(4)#3	53.6(3)
Eu(1)-O(2W)	2.492 (8)	O(7)#1-Eu(1)-O(3W)	81.5(3)
O(4)-Eu(1)#3	2.475 (8)	O(8)#2-Eu(1)-O(3W)	75.9(3)
O(8)-Eu(1)#2	2.329 (7)	O(1)-Eu(1)-O(3W)	133.6(3)
O(7)-Eu(1)#4	2.302 (7)	O(1W)-Eu(1)-O(3W)	75.2(3)
O(3)-Eu(1)#3	2.471 (8)	O(3)#3-Eu(1)-O(3W)	118.7(3)
O(7)#1-Eu(1)-O(8)#2	93.2(3)	O(4)#3-Eu(1)-O(3W)	65.3(3)
O(7)#1-Eu(1)-O(1)	141.6(3)	O(7)#1-Eu(1)-O(2W)	73.1(3)
O(8)#2-Eu(1)-O(1)	83.6(3)	O(8)#2-Eu(1)-O(2W)	76.4(3)
O(7)#1-Eu(1)-O(1W)	148.0(3)	O(1)-Eu(1)-O(2W)	69.0(3)
O(8)#2-Eu(1)-O(1W)	101.8(4)	O(1W)-Eu(1)-O(2W)	137.8(3)
O(1)-Eu(1)-O(1W)	68.9(3)	O(3)#3-Eu(1)-O(2W)	85.7(3)
O(7)#1-Eu(1)-O(3)#3	79.6(3)	O(4)#3-Eu(1)-O(2W)	131.9(3)
O(8)#2-Eu(1)-O(3)#3	162.0(4)	O(3W)-Eu(1)-O(2W)	140.9(3)
1-Tb			
Tb(1)-O(5)#1	2.285(3)	O(3W)-Tb(1)-O(1W)	75.7(3)
Tb(1)-O(6)	2.270(3)	O(6)-Tb(1)-O(10)	75.02(14)
Tb(1)-O(4)#3	2.430(3)	O(5)#1-Tb(1)-O(10)	80.34(15)

Tb(1)-O(3)#3	2.460(4)	O(2)#2-Tb(1)-O(10)	133.83(14)
Tb(1)-O(9)	2.374(3)	O(9)-Tb(1)-O(10)	75.27(15)
Tb(1)-O(2)#2	2.335(3)	O(4)#3-Tb(1)-O(10)	119.83(14)
Tb(1)-O(10)	2.431(4)	O(6)-Tb(1)-O(11)	77.42(14)
Tb(1)-O(11)	2.443(4)	O(5)#1-Tb(1)-O(11)	73.68(14)
O(2)-Tb(1)#2	2.335(3)	O(2)#2-Tb(1)-O(11)	69.22(13)
O(5)-Tb(1)#1	2.285(3)	O(9)-Tb(1)-O(11)	138.03(13)
O(3)-Tb(1)#4	2.460(4)	O(4)#3-Tb(1)-O(11)	83.74(13)
O(6)-Tb(1)-O(5)#1	92.87(13)	O(10)-Tb(1)-O(11)	140.76(15)
O(6)-Tb(1)-O(2)#2	84.40(12)	O(6)-Tb(1)-O(3)#3	141.06(13)
O(5)#1-Tb(1)-O(2)#2	142.51(13)	O(5)#1-Tb(1)-O(3)#3	74.91(14)
O(6)-Tb(1)-O(9)	101.48(15)	O(2)#2-Tb(1)-O(3)#3	127.39(12)
O(5)#1-Tb(1)-O(9)	147.23(13)	O(9)-Tb(1)-O(3)#3	75.47(13)
O(2)#2-Tb(1)-O(9)	68.93(12)	O(4)#3-Tb(1)-O(3)#3	53.55(12)
O(6)-Tb(1)-O(4)#3	160.97(14)	O(10)-Tb(1)-O(3)#3	66.61(13)
O(5)#1-Tb(1)-O(4)#3	79.12(13)	O(11)-Tb(1)-O(3)#3	130.71(12)
O(2)#2-Tb(1)-O(4)#3	91.50(12)	O(4)-Tb(1)#4	2.430(3)
O(9)-Tb(1)-O(4)#3	94.29(15)		
1-Dy			
Dy(1)-O(2)#1	2.259(6)	O(6)#2-Dy(1)-O(7)#3	90.7(2)
Dy(1)-O(1)	2.280(6)	O(3W)-Dy(1)-O(7)#3	94.5(3)
Dy(1)-O(6)#2	2.308(5)	O(2)#1-Dy(1)-O(2W)	78.2(2)
Dy(1)-O(3W)	2.355(6)	O(1)-Dy(1)-O(2W)	73.6(2)
Dy(1)-O(7)#3	2.433(6)	O(6)#2-Dy(1)-O(2W)	69.2(2)
Dy(1)-O(2W)	2.439(6)	O(3W)-Dy(1)-O(2W)	138.1(2)
Dy(1)-O(1W)	2.439(6)	O(7)#3-Dy(1)-O(2W)	83.2(2)
Dy(1)-O(8)#3	2.451(6)	O(2)#1-Dy(1)-O(1W)	75.0(2)
O(2)-Dy(1)#1	2.259(6)	O(1)-Dy(1)-O(1W)	80.1(3)
O(6)-Dy(1)#4	2.308(5)	O(6)#2-Dy(1)-O(1W)	134.3(2)
O(7)-Dy(1)#3	2.433(6)	O(3W)-Dy(1)-O(1W)	75.1(3)
O(8)-Dy(1)#3	2.451(6)	O(7)#3-Dy(1)-O(1W)	119.9(2)
O(2)#1-Dy(1)-O(1)	93.0(2)	O(2W)-Dy(1)-O(1W)	141.1(2)
O(2)#1-Dy(1)-O(6)#2	84.7(2)	O(2)#1-Dy(1)-O(8)#3	141.3(2)
O(1)-Dy(1)-O(6)#2	142.5(2)	O(1)-Dy(1)-O(8)#3	75.0(2)
O(2)#1-Dy(1)-O(3W)	100.7(3)	O(6)#2-Dy(1)-O(8)#3	126.8(2)
O(1)-Dy(1)-O(3W)	147.3(2)	O(3W)-Dy(1)-O(8)#3	75.8(2)
O(6)#2-Dy(1)-O(3W)	68.9(2)	O(7)#3-Dy(1)-O(8)#3	53.4(2)
O(2)#1-Dy(1)-O(7)#3	161.3(2)	O(2W)-Dy(1)-O(8)#3	130.0(2)
O(1)-Dy(1)-O(7)#3	79.6(2)	O(1W)-Dy(1)-O(8)#3	66.8(2)

Symmetry codes for 1-Eu: #1 x+1,y,z+1; #2 -x+2,-y+1,-z+2; #3 -x+2,-y,-z+2; #4 x-1,y,z-1.
For 1-Tb: #1 -x+1,-y,-z+1; #2 --x,-y,-z; #3 x,y-1,z; #4 x,y+1,z. For 1-Dy: #1 -x+1,-y+2,-z; #2 x-1,y,z-1; #3 -x+1,-y+1,-z; #4 x+1,y,z+1.

Table S2 Hydrogen bond geometries in the crystal structures of **1-Eu**.

Donor—H···Acceptor	D-H	H···A	D···A(Å)	D—H···A(°)
O2W—H2W1···O5	0.85	2.16	2.948(14)	155
O2W—H2W2···O7	0.85	2.53	2.851(14)	104
O2W—H2W2···O5	0.85	2.04	2.787(14)	146
O3W—H3WA···O5	0.85	2.41	2.834(14)	111
O3W—H3WB···O2	0.85	2.44	3.148(13)	141
O1W—H1W1···O1	0.85	2.43	2.715(13)	100
O1W—H1W1···O2	0.85	2.11	2.824(13)	141
O1W—H1W2···N2	0.85	1.97	2.788(15)	161
C3—H3···O3	0.93	2.49	3.078(14)	121
C6—H6B···O4	0.97	2.43	2.960(15)	114
C10—H10···O6	0.93	2.47	2.785(13)	100

Table S3 Standard Deviation (δ) calculation for the detection of Fe^{3+} for **1-Eu**.

Test	Fluorescence intensity (nm)
1	162700
2	162705
3	162702
4	162706
5	162705
6	162701
7	162702
8	162704
9	162701
10	162704
average	162703
Standard deviation (δ)	2.05

Table S4 Standard Deviation (δ) calculation for the detection of CrO_4^{2-} for **1-Eu**.

Test	Fluorescence intensity (nm)
1	101302
2	101301
3	101303
4	101302
5	101301
6	101303
7	101302
8	101302
9	101303
10	101301
average	101302
Standard deviation (δ)	0.816

Table S5 Standard Deviation (δ) calculation for the detection of $\text{Cr}_2\text{O}_7^{2-}$ for **1-Eu**.

Test	Fluorescence intensity (nm)
1	112603
2	112605
3	112603
4	112605
5	112604
6	112605
7	112603
8	112605
9	112603
10	112604
average	112604
Standard deviation (δ)	0.943

Table S6 Selected luminescent Ln-MOFs materials for sensing functionality

Name of MOF	Cations	Solvent	references
$\text{Eu}^{3+}@\text{MIL-124}$, $\{\text{MIL-124} = \text{a}_2(\text{OH})_4(\text{C}_9\text{O}_6\text{H}_4)\}$	Fe^{2+} , Fe^{3+} , $\text{Cr}_2\text{O}_7^{2-}$	H_2O	1
$[\text{H}_2\text{N}(\text{CH}_3)_2][\text{Eu}(\text{H}_2\text{O})_2(\text{BTMIPA})] \cdot 2\text{H}_2\text{O}$	Fe^{3+} , Al^{3+}	DMF	2
EuL_3	Fe^{3+}	H_2O	3
$[\text{Eu}(\text{atpt})_{1.5}(\text{phen})(\text{H}_2\text{O})]_n$	Fe^{3+} , Al^{3+}	EtOH	4
$[\text{Eu}(\text{Hpzbc})_2(\text{NO}_3)] \cdot \text{H}_2\text{O}$	Fe^{3+} , $\text{Cr}_2\text{O}_7^{2-}$	EtOH	5
$[\text{Eu}(\text{BTPCA})(\text{H}_2\text{O})] \cdot 2\text{DMF} \cdot 3\text{H}_2\text{O}$	Zn^{2+} , Fe^{3+}	DMF	6
$[\text{H}_2\text{NMe}_2]^+[\text{Eu}(\text{TCOM})]$	Fe^{3+}	H_2O	7
$[(\text{CH}_3)_2\text{NH}_2] \cdot [\text{Tb}(\text{bptc})] \cdot 0.4\text{DMF} \cdot 3.6\text{H}_2\text{O}$	Fe^{3+}	EtOH	8
$[\text{Eu}(\text{HL})(\text{H}_2\text{O})_2]_n \cdot 2\text{H}_2\text{O}$	Fe^{3+}	H_2O	9
$[\text{EuL}(\text{H}_2\text{O})_3] \cdot 3\text{H}_2\text{O} \cdot 0.75\text{DMF}$	Fe^{3+} , $\text{Cr}_2\text{O}_7^{2-}$	DMF	10
$\{[\text{Eu}_2(\text{L})_2] \cdot (\text{H}_2\text{O})_3 \cdot (\text{Me}_2\text{NH}_2)_2\}_n$	Cu^{2+} , Fe^{3+}	H_2O	11

References

- (1) Xu, X. Y.; Yan, B. Eu(III)-Functionalized MIL-124 as Fluorescent Probe for Highly Selectively Sensing Ions and Organic Small Molecules Especially for Fe(III) and Fe(II). *ACS Appl. Mater. Interfaces*, 2015, 7, 721.
- (2) Dang, S.; Ma, E.; Sun, Z. M.; Zhang, H. A layer-structured Eu-MOF as a highly selective fluorescent probe for Fe^{3+} detection through a cation-exchange approach. *J. Mater. Chem.* 2012, 22, 16920-16926.
- (3) Weng, H.; Yan, B. Lanthanide coordination polymers for multi-color luminescence and sensing of Fe^{3+} . *Inorg. Chem. Commun.* 2016, 63, 11-15.

- (4) Kang, Y.; Zheng, X. J.; Jin, L. P. A microscale multi-functional metal-organic framework as a fluorescence chemosensor for Fe (III), Al (III) and 2-hydroxy-1-naphthaldehyde. *J. Colloid Interface Sci.* 2016, **471**, 1-6.
- (5) Li, G. P.; Liu, G.; Li, Y. Z.; Hou, L.; Wang, Y. Y.; Zhu, Z. Uncommon pyrazoyl-carboxyl bifunctional ligand-based microporous lanthanide systems: sorption and luminescent sensing properties. *Inorg. Chem.* 2016, **55**, 3952-3959.
- (6) Tang, Q.; Liu, S.; Liu, Y.; Miao, J.; Li, S.; Zhang, L.; Zheng, Z. Cation sensing by a luminescent metal-organic framework with multiple Lewis basic sites. *Inorg. Chem.* 2013, **52**, 2799-2801.
- (7) Lu, W. G.; Jiang, L.; Feng, X. L.; Lu, T. B. Three-dimensional lanthanide anionic metal-organic frameworks with tunable luminescent properties induced by cation exchange. *Inorg. Chem.* 2009, **48**, 6997-6999.
- (8) Zhao, X. L.; Tian, D.; Gao, Q.; Sun, H. W.; Xu, J.; Bu, X. H. A chiral lanthanide metal-organic framework for selective sensing of Fe (III) ions. *Dalton Trans.* 2016, **45**, 1040-1046.
- (9) Liang, Y. T.; Yang, G. P.; Liu, B.; Yan, Y. T.; Xi, Z. P.; Wang, Y. Y. Four super water-stable lanthanide-organic frameworks with active uncoordinated carboxylic and pyridyl groups for selective luminescence sensing of Fe³⁺. *Dalton Trans.* 2015, **44**, 13325-13330.
- (10) Gao, R. C.; Guo, F. S.; Bai, N. N.; Wu, Y. L.; Yang, F.; Liang, J. Y.; Wang, Y. Y. Two 3D Isostructural Ln (III)-MOFs: Displaying the Slow Magnetic Relaxation and Luminescence Properties in Detection of Nitrobenzene and Cr₂O₇²⁻. *Inorg. Chem.* 2016, **55**, 11323-11330.
- (11) Chen, Z.; Sun, Y.; Zhang, L.; Sun, D.; Liu, F.; Meng, Q.; Sun, D. A tubular europium-organic framework exhibiting selective sensing of Fe³⁺ and Al³⁺ over mixed metal ions. *Chem. Commun.* 2013, **49**, 11557-11559.

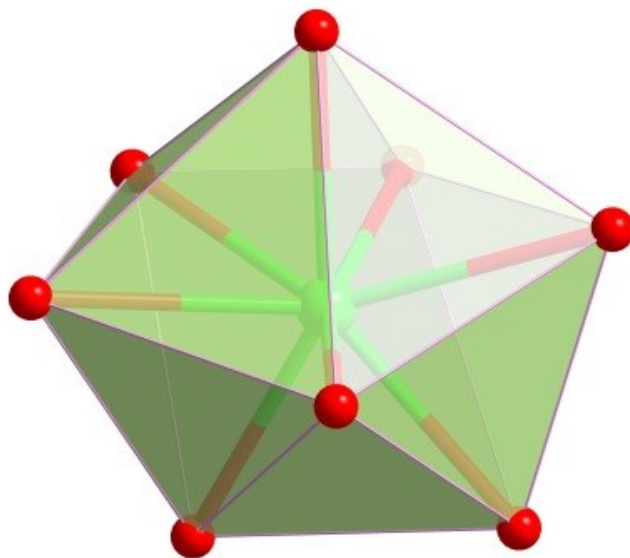


Fig. S1 Coordination arrangement of Eu^{3+} ion could be described as a distorted hendecahedron.

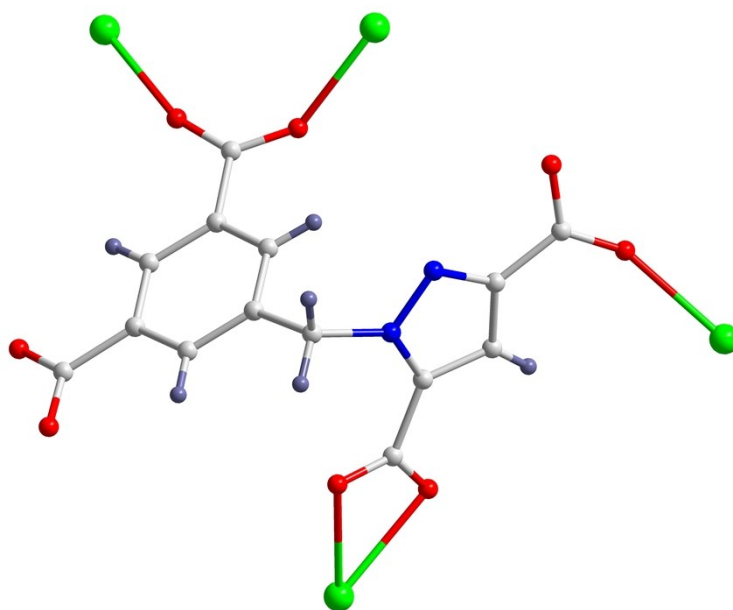


Fig. S2 The three carboxylates of HL^{3-} ligands take coordination with Eu^{3+} ions.

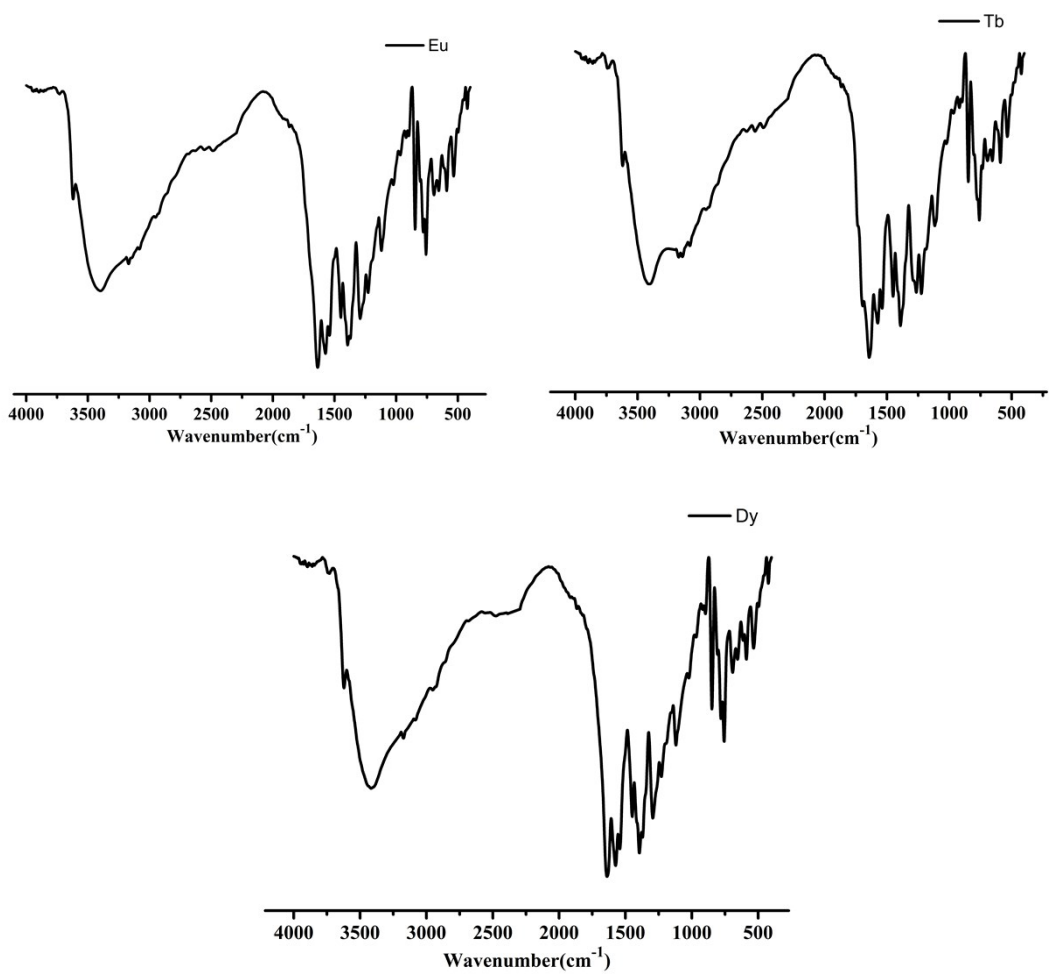
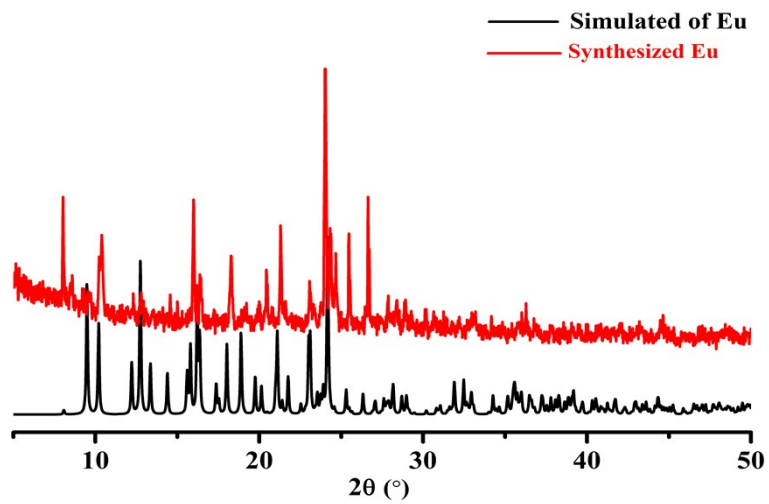


Fig. S3 The FT-IR spectrometer of 1-Eu, 1-Tb and 1-Dy.



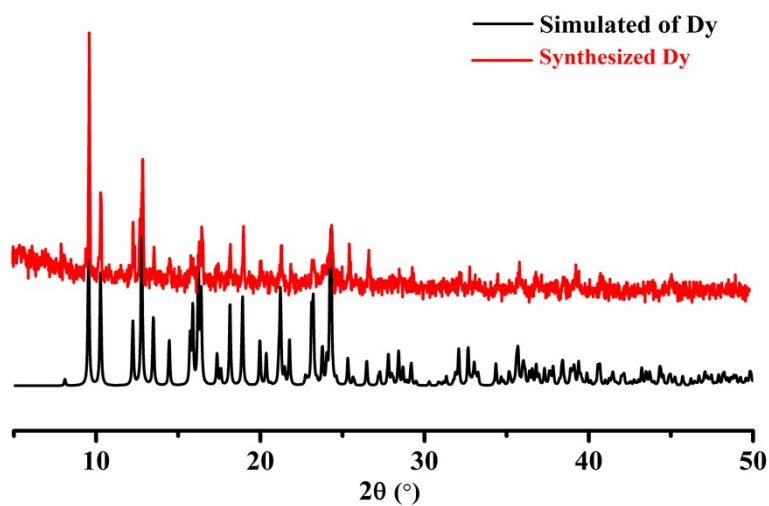
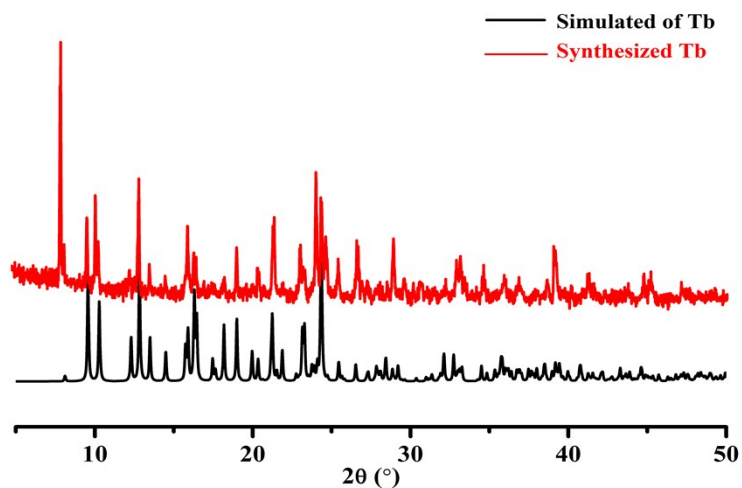


Fig. S4 PXRD patterns of **1-Eu**, **1-Tb** and **1-Dy** simulated from the X-ray single-crystal structure and as-synthesized samples of **1-Eu**, **1-Dy** and **1-Tb**.

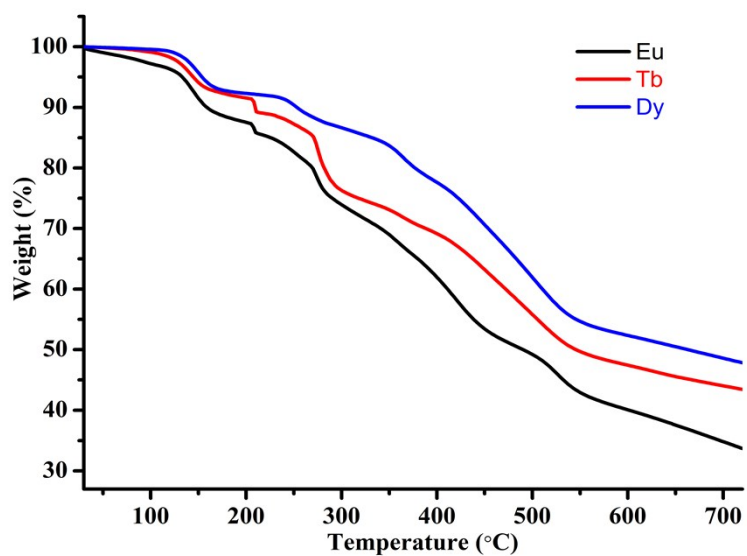


Fig.S5 The TGA plots of three compounds under N₂ environment. For **1-Tb**, the first major weight loss of 10.89% from 30 to 214°C, corresponding to three coordinated water (calca.10.07%), the major framework can keep stable to 268°C. For **1-Dy**, the first major weight loss of 8.16% from 30 to 175°C, ascribing to three coordinated water, (calca.9.92%), the major framework can keep stable to 233°C.

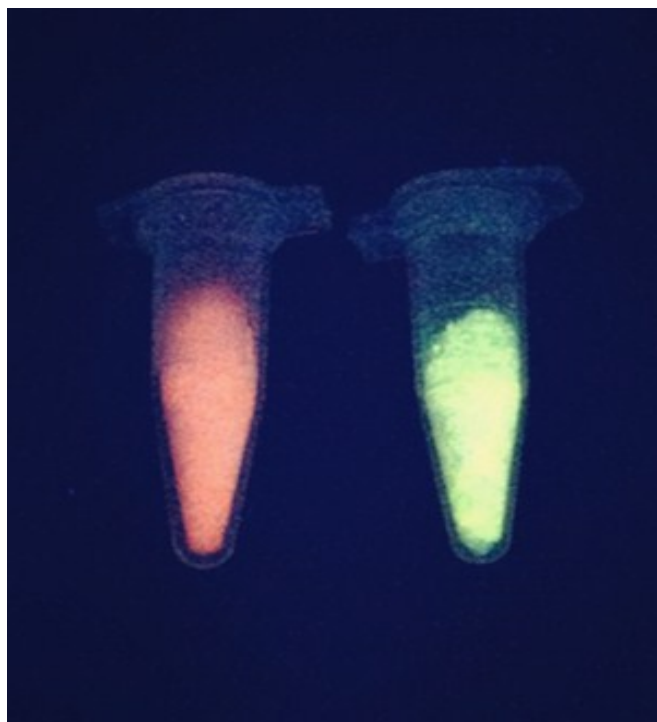


Fig. S6 Snapshots of **1-Eu** (left) and **1-Tb** (right) under UV light (365 nm).

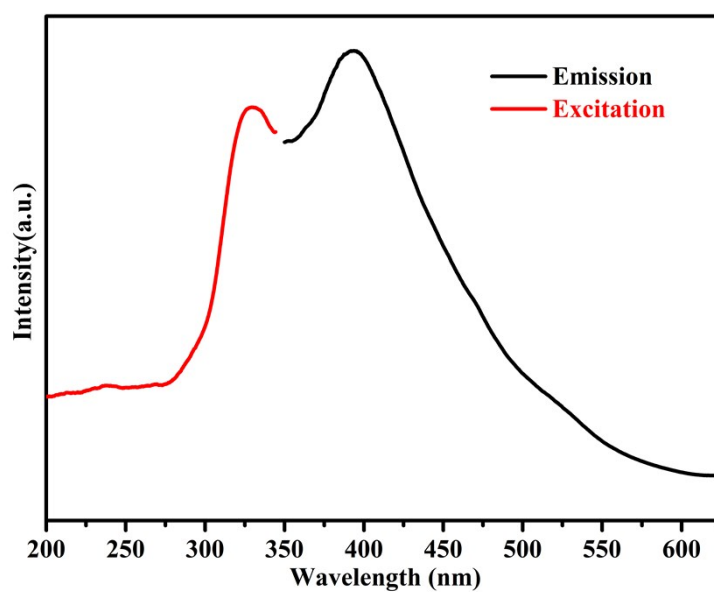
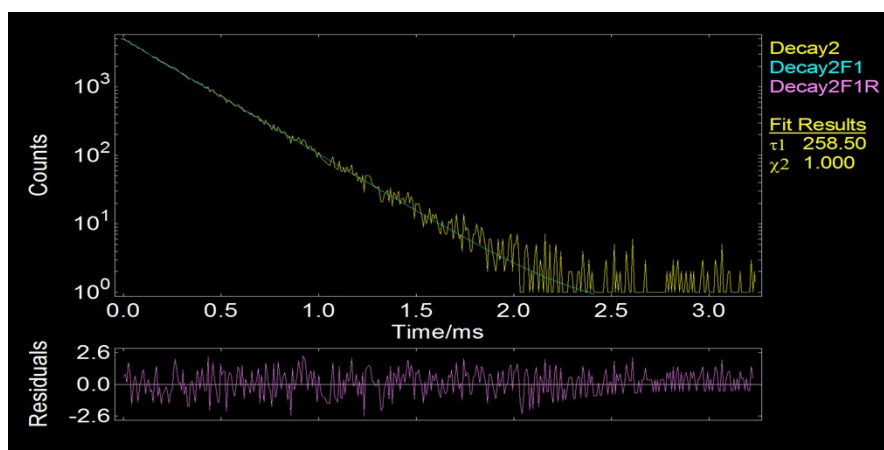
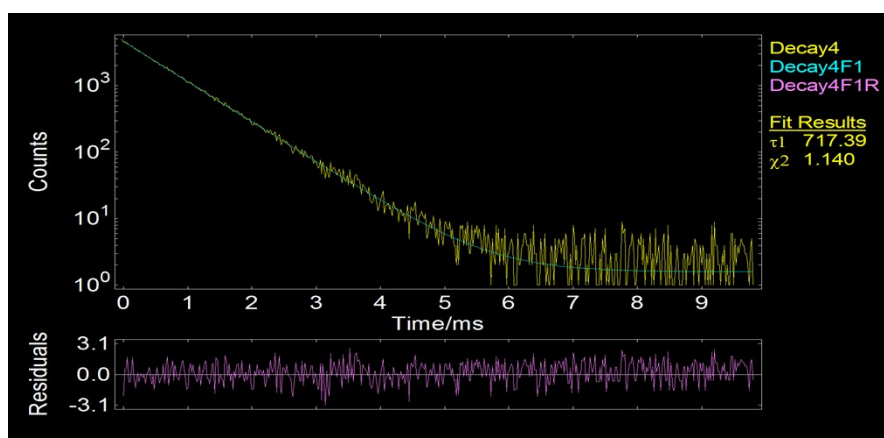


Fig. S7 The Excitation and emission spectra of H₄L

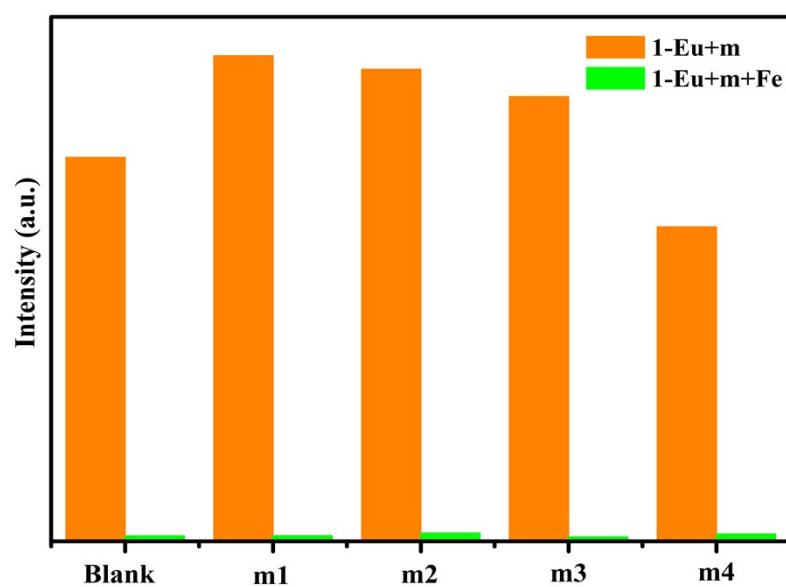


(a)

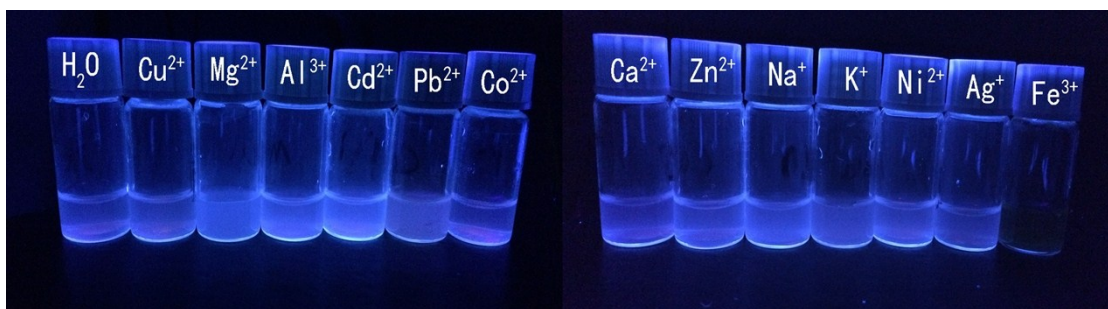


(b)

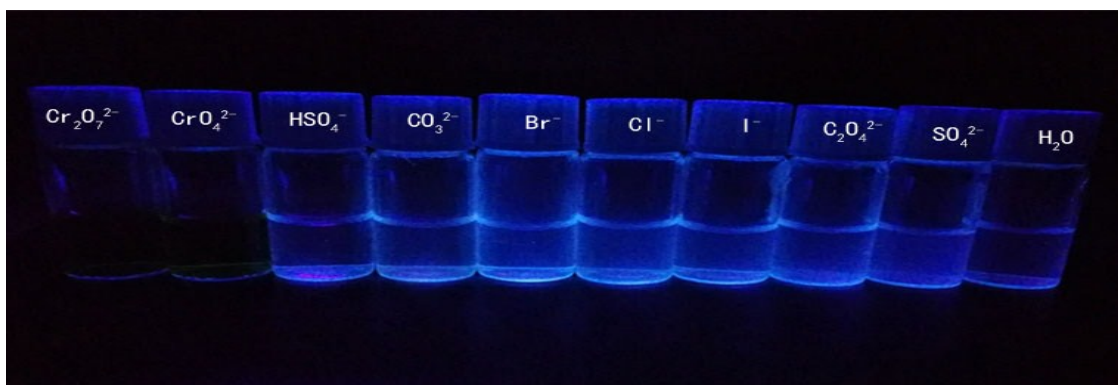
Figure S8. Luminescence decay of **1-Eu (a)** and **1-Tb (b)** measured at the excitation/emission maxima, which can be fitted with exponential decay: **(a)** $\tau_1 = 258.50 \mu\text{s}$ (5.04%), $\chi^2 = 1.000$; **(b)** $\tau_1 = 717.39 \mu\text{s}$ (15.12%), $\chi^2 = 1.140$.



(a)

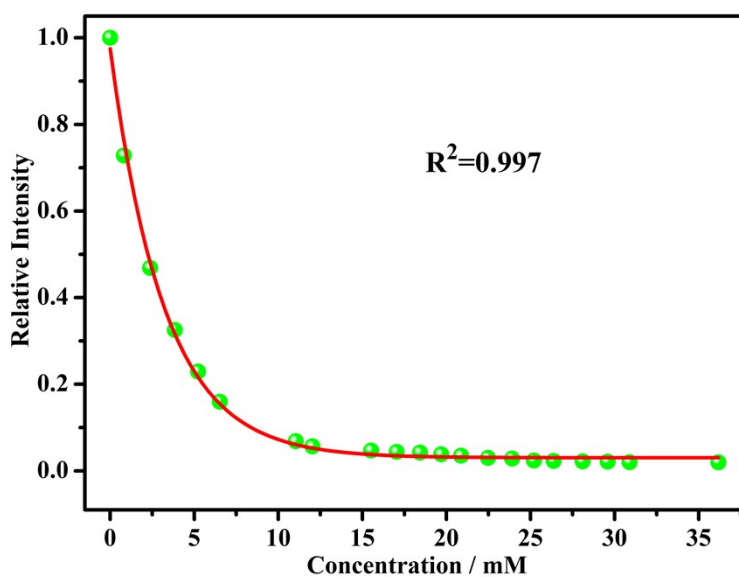


(b)

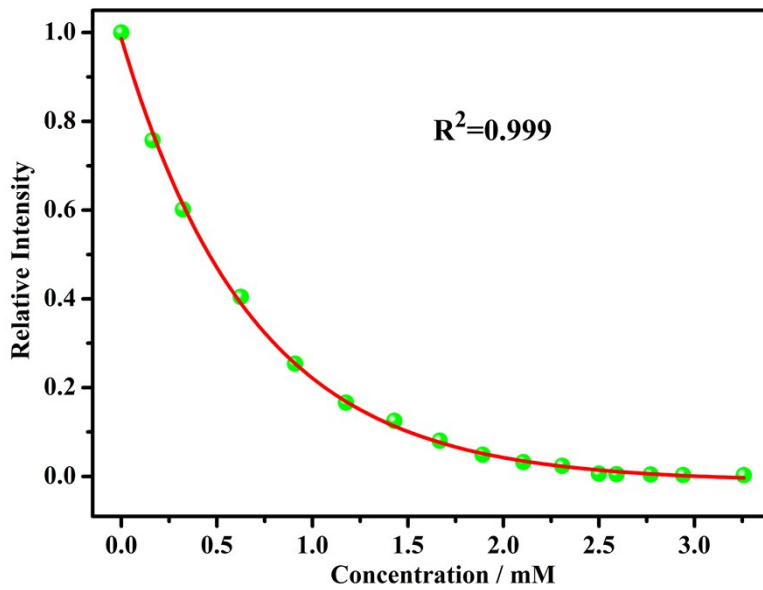


(c)

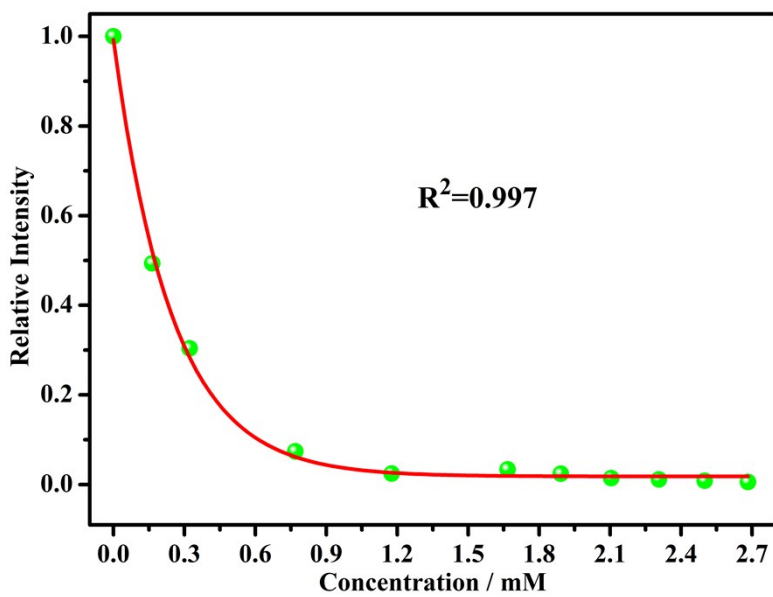
Fig. S9 (a) Luminescence intensity at 615 nm of **1-Eu** dispersed in water with addition of different mixed ions (10^{-2} M) mixed solution added Fe^{3+} ions (10^{-2} M) (m1: $\text{Co}^{2+}/\text{Ca}^{2+}$; m2: $\text{Na}^{+}/\text{K}^{+}/\text{Mg}^{2+}$; m3: $\text{Al}^{3+}/\text{Ni}^{2+}/\text{Pb}^{2+}$; m4: $\text{Ag}^{+}/\text{Ca}^{2+}/\text{Cd}^{2+}/\text{Zn}^{2+}$). (b) Pictures of different $\text{Mn}^{+}@\mathbf{1-Eu}$ solutions ($\text{M} = \text{Cu}^{2+}, \text{Mg}^{2+}, \text{Al}^{3+}, \text{Cd}^{2+}, \text{Pb}^{2+}, \text{Co}^{2+}, \text{Ca}^{2+}, \text{Zn}^{2+}, \text{Na}^{+}, \text{K}^{+}, \text{Ni}^{2+}, \text{Ag}^{+}$ and Fe^{3+} , respectively). (c) Pictures of different $\mathbf{1-Eu}@A^{n-}$ solutions ($A = \text{Cr}_2\text{O}_7^{2-}, \text{CrO}_4^{2-}, \text{HSO}_4^{-}, \text{CO}_3^{2-}, \text{Br}^{-}, \text{Cl}^{-}, \text{I}^{-}, \text{C}_2\text{O}_4^{2-}$ and SO_4^{2-} , respectively).



(a) Fe^{3+}

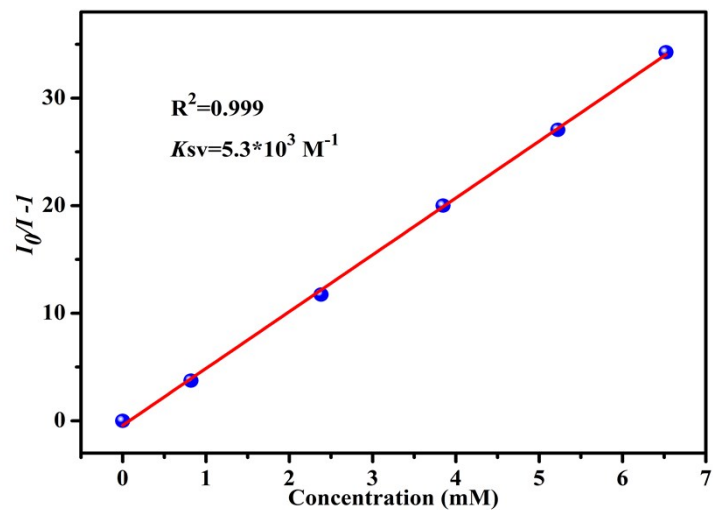


(b) CrO_4^{2-}

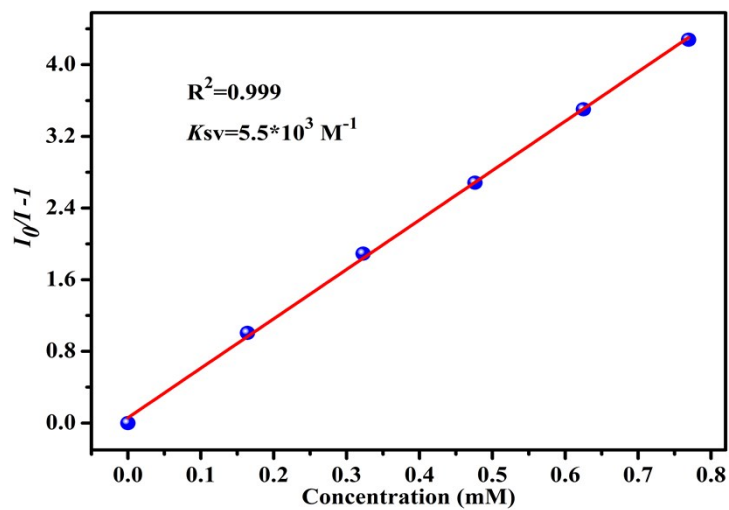


(c) $\text{Cr}_2\text{O}_7^{2-}$

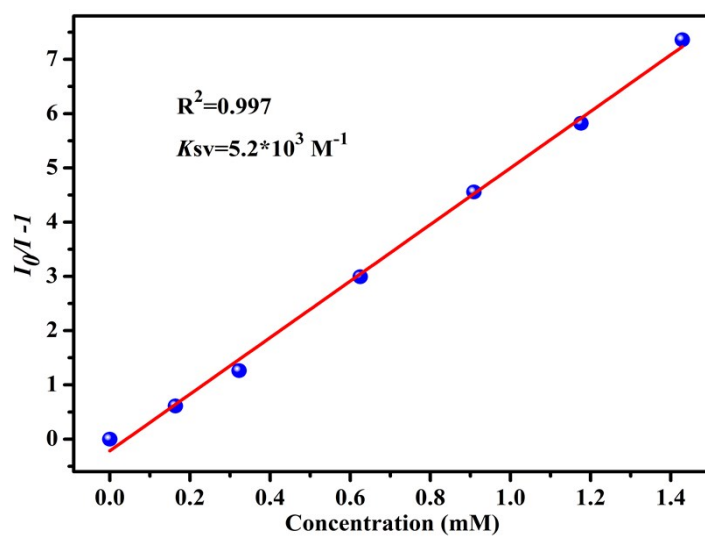
Figure S10 The linear correlation for the plot of I_0/I vs concentration of Fe^{3+} (a) , CrO_4^{2-} (b) and $\text{Cr}_2\text{O}_7^{2-}$ (c) ions, respectively, in low concentration range.



(a) Fe^{3+}



(b) $\text{Cr}_2\text{O}_7^{2-}$



(c) CrO_4^{2-}

Fig. S11 Quenching efficiency defined by the Stern–Volmer relationship for Fe^{3+} , $\text{Cr}_2\text{O}_7^{2-}$ and CrO_4^{2-} ions.

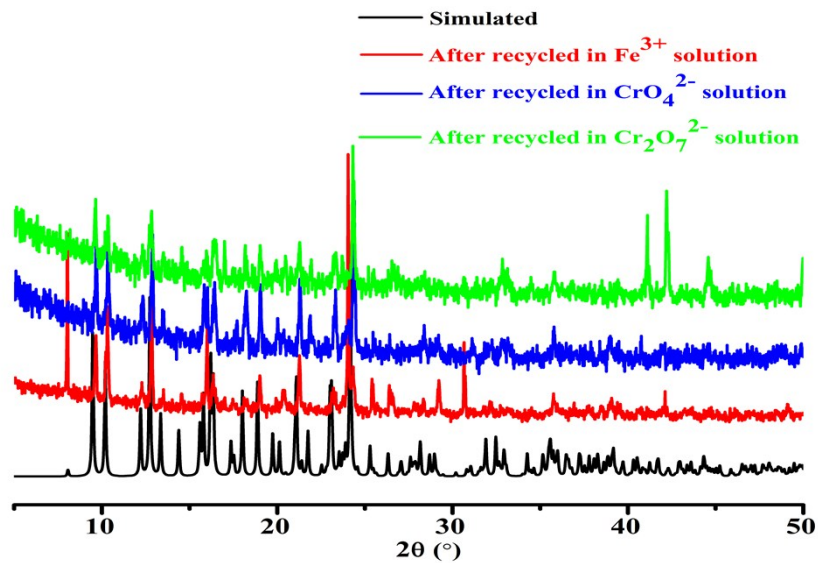


Fig. S12 The PXRD patterns of **1-Eu** treated by Fe^{3+} , CrO_4^{2-} and $\text{Cr}_2\text{O}_7^{2-}$ aqueous solutions.

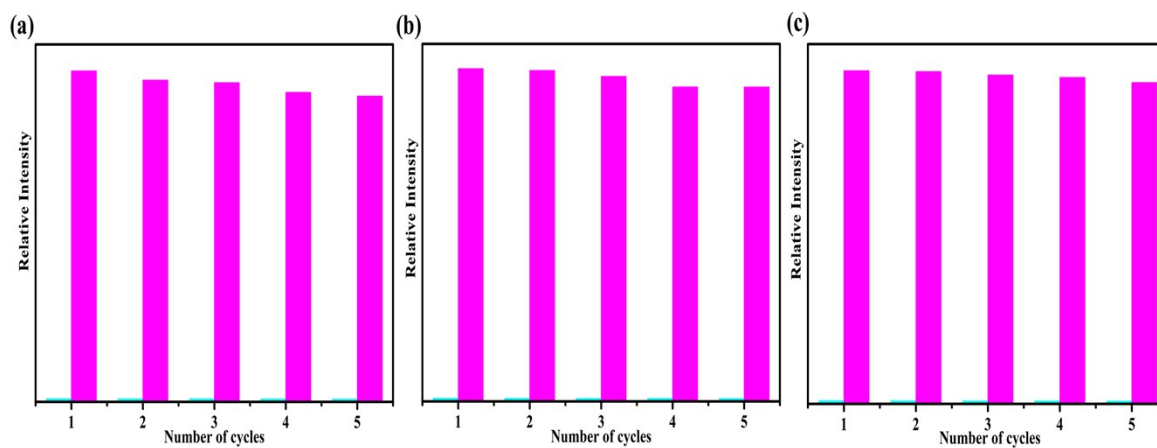


Fig. S13 Luminescent intensity at 615 nm of **1-Eu** after five recycles in Fe^{3+} , $\text{Cr}_2\text{O}_7^{2-}$ and CrO_4^{2-} solutions (10^{-2} M).

Sample	Concentration of Eu^{3+} ($\mu\text{g/mL}$)
Blank sample (H_2O)	0.0176
Initial solution after immersing in H_2O	0.0208
Final solution after recycle sensing experiment for Fe^{3+}	0.0198
Final solution after recycle sensing experiment for CrO_4^{2-}	0.0201
Final solution after recycle sensing experiment for $\text{Cr}_2\text{O}_7^{2-}$	0.0194

Fig. S14 ICP experiments of **1-Eu** after immersing in different solution.

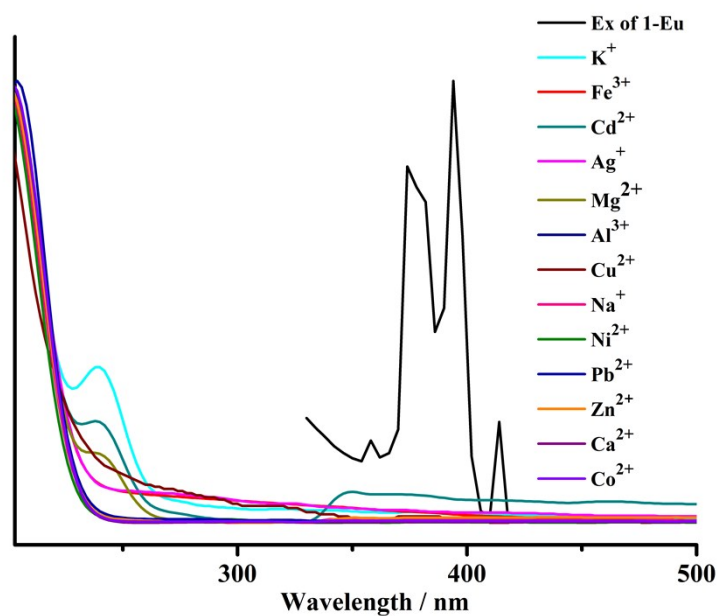


Fig. S15 UV-Vis adsorption spectrum of $\text{M}(\text{NO}_3)_x$ aqueous solution and the excitation spectrum of **1-Eu**.

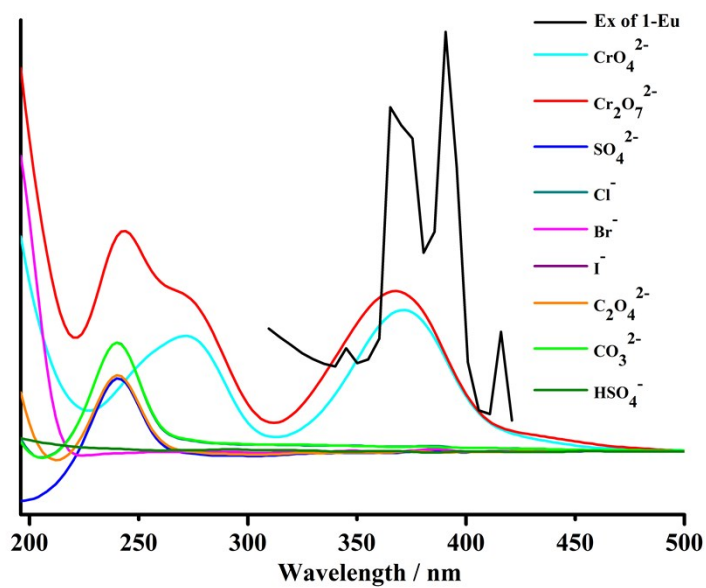


Fig. S16 UV-Vis adsorption spectrum of K_x(A) aqueous solution and the excitation spectrum of 1-Eu.

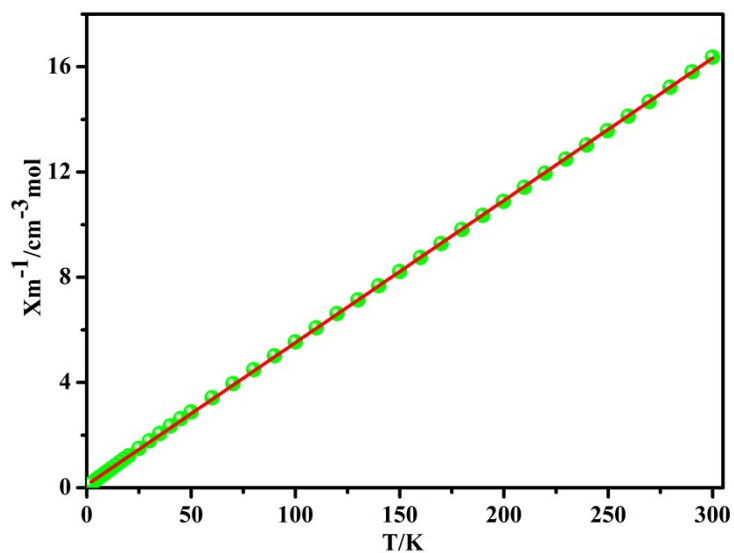


Fig. S17 The inverse magnetic susceptibility data (χM^{-1}) of 1-Dy.